The kinetics of CO oxidation by adsorbed oxygen on well-defined gold particles on TiO_2(110)

Victor A. Bondzie, Stephen C. Parker and Charles T. Campbell *

Department of Chemistry, Box 351700, University of Washington, Seattle, WA 98195-1700, USA

Received 14 July 1999; accepted 25 August 1999

Very tiny Au particles on TiO_2 show excellent activity and selectivity in a number of oxidation reactions. We have studied the vapor deposition of Au onto a TiO_2(110) surface using XPS, LEIS, LEED and TPD and found that we can prepare Au islands with controlled thicknesses from one to several monolayers. In order to understand at the atomic level the unusual catalytic activity in oxidation reactions of this system, we have studied oxygen adsorption on Au/TiO_2(110) as a function of Au island thickness, and have measured the titration of this adsorbed oxygen with CO gas to yield CO_2, as function of Au island thickness, CO pressure and temperature. A hot filament was used to dose gaseous oxygen atoms. TPD results show higher O_2 desorption temperatures (741 K) from ultrathin gold particles on TiO_2(110) than from thicker particles (545 K). This implies that O_a bonds much more strongly to ultrathin islands of Au. Thus from Brønsted relations, ultrathin gold particles should be able to dissociatively adsorb O_2 more readily than thick gold particles. Our studies of the titration reaction of oxygen adatoms with CO (to produce CO_2) show that this reaction is extremely rapid at room temperature, but its rate is slightly slower for the thinnest Au islands. Thus the association reaction ($CO_g + O_a \rightarrow CO_{2,g}$) gets faster as the oxygen adsorption strength decreases, again as expected from Brønsted relations. For islands of about two atomic layers thickness, the rate increases slowly with temperature, with an apparent activation energy of 11.4 ± 2.8 kJ/mol, and shows a first-order rate in CO pressure and oxygen coverage, similar to bulk Au(110).

Keywords: gold, TiO_2, model catalysts, CO oxidation, support effects

1. Introduction

As compared to more traditional catalysts (Pt, Pd, Rh), bulk gold is typically regarded as catalytically inert. This is because pure gold is known to be unreactive to most gases including CO and O_2. However, it has been found most recently that when gold is deposited on reducible metal oxides such as TiO_2, Fe_2O_3, Co_3O_4 as ultrafine particles, there is a remarkable change in its catalytic activity [1–3]. For example, highly dispersed gold particles supported on metal oxides such as TiO_2 have been reported to be extremely active for reactions including partial oxidation of hydrocarbons, reduction of nitrogen oxides, low-temperature CO oxidation and propene epoxidation [1–4]. This ability of supported gold on TiO_2 to act as a catalyst for the room-temperature oxidation of CO shows exciting potential in automotive applications, CO detection devices and purification of air in homes and offices.

The activity of Au catalysts in these oxidation reactions is somewhat surprising, since dissociatively adsorbed oxygen is generally thought to be the active oxidant in related reactions on other noble metals. This is in spite of the fact that molecular O_2 is known not to dissociatively adsorb on bulk gold at pressures as high as 1400 Torr and temperatures between 300 and 500 K [5,6]. Various mechanisms have been proposed for CO oxidation on supported Au catalysts [7–9]. The mechanism for the catalytic CO oxidation on the Au/TiO_2 catalyst is still not well understood, with many questions remaining on the site of the reaction and the nature of interaction between the gold particles and the TiO_2 metal substrate. One mechanism suggested for CO oxidation on the Au/TiO_2 catalyst is a Langmuir–Hinshelwood model invoking CO weakly adsorbed on Au which reacts with oxygen activated at the Au/TiO_2 interface [2–4]. This model suggests that the presence of gold clusters on the TiO_2 leads to the dissociative adsorption of oxygen at the Au/TiO_2 interface, which has led to other studies that have attempted to clarify whether new adsorption sites are really created on the Au/TiO_2 catalyst that interact with molecular oxygen [9–11]. No such sites were identified spectroscopically [9–11]. In the proposed mechanism for room-temperature CO oxidation on Au/ZnO, oxidic gold sites have been identified as the active species, and the ZnO substrate was proposed to mainly stabilize the gold particles in a highly dispersed form capable of adsorbing oxygen and CO [8].

The role of the metal oxide supports in the catalytic activity of gold in CO oxidation has also been investigated by Okumura et al. [12]. They found the catalytic activities of Au/SiO_2, Au/Al_2O_3 and Au/TiO_2 to be similar particularly for small clusters of Au [12], i.e., independent of the support. This indicates that the catalytic activity for these nanoparticles of Au on TiO_2 is essentially determined by the intrinsic electronic structure of the gold clusters. Further investigation by Goodman's group [13,14] has unambiguously shown that the reaction kinetics for the catalytic CO oxidation on Au/TiO_2 is strongly dependent on the Au clus-

* To whom correspondence should be addressed.

ter size. They have demonstrated from scanning tunnelling microscopy/spectroscopy (STM/STS) and reaction kinetic measurements that the reactivities of the Au/TiO_2 system for CO oxidation are defined by changes of the electronic properties of the Au clusters which vary with the size of the Au clusters, optimizing at clusters with thicknesses of two atomic layers [13,14].

In order to further understand the mechanism of the catalytic oxidation on gold supported on TiO_2 at the molecular level, we have studied the vapor deposition of gold onto a $TiO_2(110)$ surface, using XPS and LEIS [15]. The Au was found to grow first in islands of single-atom thickness (i.e., two-dimensional or 2D islands). These 2D islands spread to cover ∼10% of the surface as Au deposition proceeds. Above this critical coverage of ∼0.10 ML, the growth mode switches, and further Au adds mainly *on top* of the existing islands, to make thicker and thicker 3D islands as coverage increases. Thus, the island thickness could be controlled from one atomic layer upwards by increasing the Au coverage from ∼0.10 ML. Upon annealing, the Au islands irreversibly thicken, uncovering part of the TiO_2. This proves that the Au thermodynamically prefers 3D islands (Volmer–Weber growth), and the 2D islands are a less stable structure. Qualitatively similar growth behavior has been reported previously [10,16].

We also studied the adsorption and desorption of oxygen from these well-defined Au particles [17]. A hot filament was used to generate gaseous oxygen atoms, which adsorbed to produce oxygen adatoms. This technique has been used previously to produce oxygen overlayers on bulk Au(110) surfaces [5,6]. An increasing desorption temperature for $2O_a \rightarrow O_{2,g}$ showed that the O–Au chemisorption bond strength on thin gold islands is greater than on thick gold islands [17]. Brønsted relations [18] predict that the activation barrier for dissociative adsorption of O_2 should be lower for gold particles with a higher adsorption energy for oxygen adatoms. Thus, ultrathin gold particles should be able to dissociatively adsorb O_2 more readily than large gold particles. Since dissociative adsorption of O_2 is impossible on pure, bulk gold surfaces, we have postulated that the unusual low-temperature catalytic activity in CO oxidation demonstrated by thin (small) Au particles on TiO_2 is related to the positive influence that this stronger bonding to oxygen will no doubt have on the dissociative adsorption rate of O_2. So far, we have been unable to experimentally demonstrate this, since the rate of O_2 adsorption is very slow in any case (and probably rate limiting in the catalytic process). Under conditions where we should have observed it, the adsorbed oxygen would have been rapidly cleaned off by reactions with low-level background impurities, so we are striving to make the measurement in a cleaner environment.

In this paper, we further study oxygen adsorption on 2D and 3D gold islands as a function of thickness, and also measure the titration of this adsorbed oxygen with CO gas to yield CO_2, as a function of Au island thickness, CO pressure and temperature. This titration reaction is found to be extremely rapid at room temperature. This proves that, if O_a on the Au particles is an intermediate in low-temperature CO oxidation, its production must be rate limiting, since its consumption by CO is so fast. The titration rate increases as island thickness increases from 2D to 3D Au islands. Thus, the association reaction ($CO_g + O_a \rightarrow CO_{2,g}$) gets faster as the oxygen adsorption energy decreases.

2. Experimental

The experiments were conducted in an ultrahigh vacuum (UHV) system described previously [19,20]. Briefly, the system consists of three sections: a microreactor for high-pressure adsorption experiments and two adjacent UHV chambers I and II with a base pressure of $\sim 4 \times 10^{-10}$ mbar. Chamber I is equipped with LEED while chamber II is equipped with facilities for XPS, LEIS, LEED and TPD. The TiO_2 sample could rapidly be transferred between the various sections of the UHV system. The polished and oriented $TiO_2(110)$ single crystal was obtained from Commercial Crystal Laboratories, Inc. A chromel–alumel thermocouple was directly glued (using Aremco high-temperature cement) to the TiO_2 crystal which was mounted on a tantalum sample holder. The sample was heated resistively and, for TPD, a heating rate of 4.5 K/s was used. Preparation and cleaning of the $TiO_2(110)$ single crystal which produces a stoichiometric surface has been described elsewhere ([21] and references therein). All XPS measurements were performed with Al Kα X-rays and detection normal to the surface, and all LEIS measurements were recorded with 1.25 keV He^+ ions, with an ion current of 0.2 μA/cm^2. Ion exposure times were ∼270 s for a typical LEIS spectrum.

The well-defined Au clusters were obtained by vapor deposition at room temperature via a resistively heated doser containing high-purity (99.95%) gold foils, as described in [15,17]. The TiO_2 sample's temperature rose by ∼20–80 K during the period of gold deposition due to radiation from the source. The XPS intensity ratio of the Au $4f_{7/2}$ (I_{Au}) to the initial or clean Ti $2p_{3/2}$ peaks (I^0_{Ti}) was used to determine Au coverages and calibrated, as described in [15,17], based on combined measurements of XPS and LEIS versus coverage and known escape depths for photoelectrons. LEIS measurements were mainly used to calculate the fractional area (f_{Au}) of the $TiO_2(110)$ surface covered with Au islands, from the attenuation of the Ti LEIS peak intensity and from the Au LEIS intensity (relative to pure multilayer Au), also as described in [15,17]. By combining the XPS and LEIS measurements, the average thickness of the gold clusters could be determined. This will be reported in units of atomic layers, with each atomic layer corresponding to 2.35 Å (the interlayer spacing between Au(111) planes in bulk Au, and thus 1.39×10^{15} Au atoms per cm^2 of island area).

Research grade purity CO and O_2 obtained from AirCo was used. The gas purity was further checked by mass spectroscopy. As mentioned earlier, atomic oxygen gas was

dosed by facing the Au/TiO_2 sample towards the mass spectrometer ion source, and introducing O_2 gas with the mass spectrometer filament on. Details are the same as in [6,17]. To obtain coverages of oxygen adatoms (O_a) of $\sim$0.35 ML, we used an O_2 pressure of $\sim 2 \times 10^{-5}$ mbar and an exposure time of 120 min. LEIS measurements of the attenuation of the Au signal by O_a were further used to estimate the coverages of the O_a overlayer on the Au particles. The accuracy of this method was confirmed by comparison to the O_2 TPD peak areas [17]. We define 1.0 ML of O_a on the Au islands as that oxygen coverage which would lead to 100% attenuation of the Au LEIS signal. The saturation coverage of O_a obtained on Au(110)-(1 $\times$ 2) in this same way also using He LEIS to measure coverage was 0.95 ML, and it corresponds to $\sim 1.5 \times 10^{15}$ oxygen adatoms per cm^2 [22]. Controlled LEIS experiments showed that these LEIS measurements resulted in little or no ion beam damage to the sample and negligible removal of O_a or Au. Subsequent to these measurements the sample was heated to desorb the adsorbed atomic oxygen species, and the O_2 TPD peak areas were not diminished due to ion doses exceeding those used here.

Similar to the TPD experiments, the CO titration experiments involved initially dosing the Au/TiO_2(110) surface with oxygen ($P_{O_2} \approx 2 \times 10^{-5}$ mbar for 120 min) at room temperature using the hot filament technique to yield reasonable coverages of O adatoms characterized by LEIS. The reaction kinetics were then followed by two methods. The first method involved immediately introducing the initially O-covered Au/TiO_2 surface to CO at a constant leak rate. The transient responses of m/e 28 (CO) and 44 (CO_2) were then followed with a mass spectrometer. The CO_2 production rate $R_{CO_2}(t)$ was determined throughout the titration from the increase in the CO_2 pressure above the background. However, because of a large and difficult to estimate background correction needed with this method, reaction kinetics in this report will be quantified mainly by a second method. This consisted of periodic interruptions of the CO flow (by closing the CO leak valve) and measurements by LEIS of the O-covered Au/TiO_2 surface, again using the attenuation of the Au peak to quantify O_a coverages. Again, control experiments using O_2 TPD peak areas to assess the residual O_a coverage confirmed the accuracy of this LEIS method. Finally, the slope of the oxygen coverage (θ_O) versus exposure time to CO was used to determine the CO_2 production rate ($dCO_2/dt = -d\theta_O/dt$) or the net reaction ($CO_g + O_a \rightarrow CO_{2,g}$) rate.

3. Results

3.1. TPD results of O adatoms on Au/TiO2(110)

Figure 1 shows associative desorption of oxygen adatoms as O_2 as a function of Au island thickness. Though this experiment is largely a repetition of our earlier published work [17], it contains new results in that the temperature

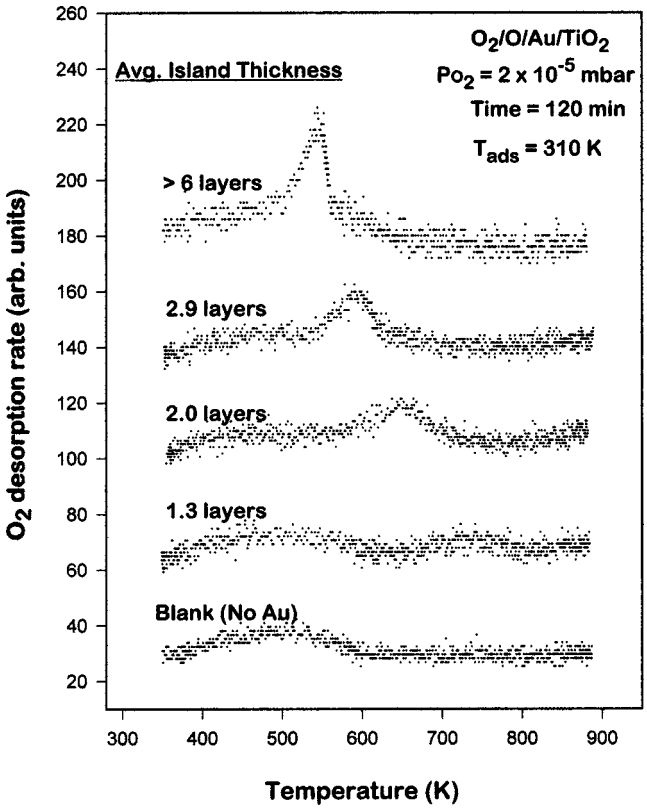

Figure 1. O_2 TPD curves for 0.35 ML of oxygen adatoms on Au islands of different average thicknesses in atomic layers. These islands covered the following fractions of the TiO_2(110) surface: 14% (1.3 layers), 28% (2.0 layers), 43% (2.9 layers) and 60% (>6 layers).

ramp extends up to 880 K. This allows one to see oxygen desorption from 2D islands ($\sim$1.3-atomic layers thick) not seen in an early TPD which extended only to 710 K. Here, the O_2 exposure was 2.4×10^{-3} mbar min, in front of the hot filament. The effect of the Au island thickness on the oxygen TPD spectra following such exposures to atomic oxygen gas is similar and consistent with what we have reported in [17]. All the essential features including Au island thickness and desorption temperature maxima are reproduced in these results. The island thicknesses reported here refer to the metal film as dosed at 310 K, prior to the deposition or desorption of the oxygen adatoms. We observed that the Au clusters thicken further upon heating above 500 K in the absence of O_a, as also seen by other groups [10,16]. Therefore, as stated earlier in [17], the island thickness shown here should be viewed as a qualitative initial average thickness at the specified initial temperatures. Since oxygen adsorbs strongly to the gold but not to the TiO_2, its presence is expected to inhibit island thickening [26]. From the attenuation of the Au LEIS intensity, this oxygen exposure used here produces about the same coverage of oxygen adatoms ($\sim$0.35 ML) on the various islands of Au on TiO_2(110), irrespective of their thickness. Note that the TPD peak areas increase as the particle thickness increases. This is only because the fraction of the surface covered by the Au islands (reported in the caption to figure 1) is correspondingly increasing. Clearly

we observe the highest TPD peak temperature (741 K) for the thinnest Au islands (∼1.3 layers thick). It gradually shifts to lower temperatures as the particle thickness increases, up to islands of thickness of at least ∼6-atomic layers.

A single, sharp O_2 desorption peak, with a maximum at 545 K, is observed from the multilayer gold cluster (>6 layers). This is in contrast to the broadened peak with two major maxima (one occurring at 545 K and the other at 520 K) observed in our earlier findings for the same Au coverage which had been pre-annealed to ∼670 K [17]. This broadened peak was ascribed to heterogeneous Au sites offered by the pre-annealed Au adlayer [17]: a less strongly bound state for O_a (at 520 K) and strongly bound state (at 545 K). The strongly bound state is shown here to dominate for Au particles not pre-annealed, which appear more homogeneous in such sites. The 520 K desorption peak for the annealed film suggests the presence of some Au islands that are thicker (larger), likely arising from the thermal thickening or sintering of the Au particles. A blank experiment (bottom trace) from the bare TiO_2(110) surface (with no deposited Au particles) showed a broad peak feature between 430 and 570 K, which represents background O_2 desorption from the sample holder and/or the TiO_2(110) surface.

3.2. Titration experiments: $CO_g + O_a \rightarrow CO_{2,g}$

We have used the attenuation of the Au LEIS intensity here to probe the removal of adsorbed oxygen on the Au/TiO_2(110) surface by CO gas. We have shown elsewhere [6] that the O coverage (as probed by the O_2 TPD peak area) is proportional to the attenuation of the Au LEIS intensity. Figure 2 shows the LEIS signal of O-covered Au on TiO_2(110) as a function of CO dose at room temperature. The top and bottom spectra represent the Au LEIS intensities of the clean 3D Au islands on TiO_2(110) and these same islands after preadsorbing ∼0.40 ML O_a on them, respectively. Note that this O_a attenuates the Au LEIS signal by ∼40%. Upon exposures to CO, the Au LEIS intensity increases correspondingly back toward its oxygen-free value, indicating the removal of the O_a with CO according to the titration reaction: $CO_g + O_a \rightarrow CO_{2,g}$. From our controlled experiments the disappearance of the atomic oxygen is not attributable to the presence of any background hydrogen in the UHV chamber since the reaction between H_2 and oxygen adatoms on gold has also been shown to be negligible under UHV conditions [6].

Figure 3 shows the mass spectrometer signal of the evolution of CO_2 gas due to this titration reaction of O_a with CO gas at room temperature. The trace of the CO_2 curve

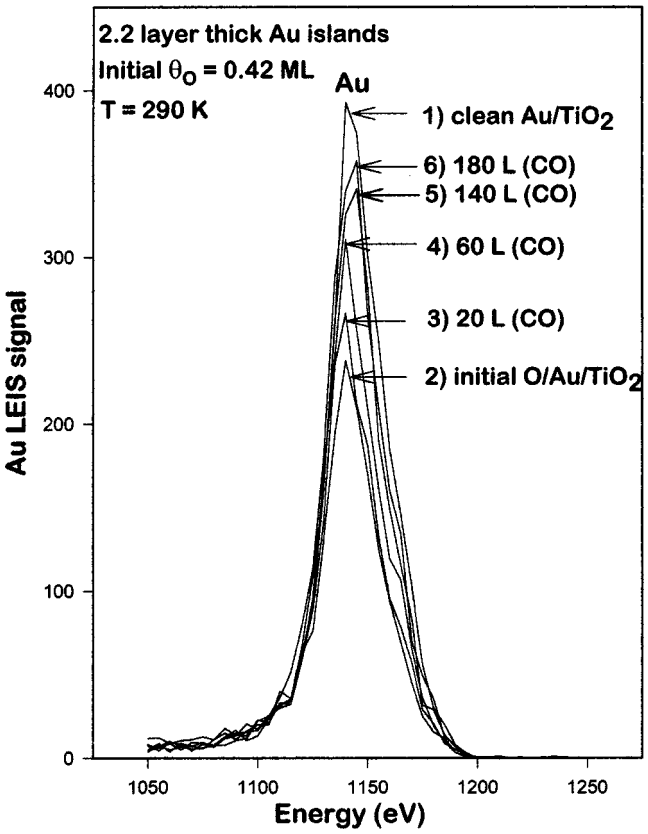

Figure 2. Evolution of the Au LEIS signal during the course of a typical titration experiment at doses at room temperature (290 K). The top (1) and bottom (2) traces are the clean and initially O-covered Au LEIS signals, respectively. The reaction: $CO_g + O_a \rightarrow CO_{2,g}$, causes the increase in Au LEIS signal going from curves (2) → (6).

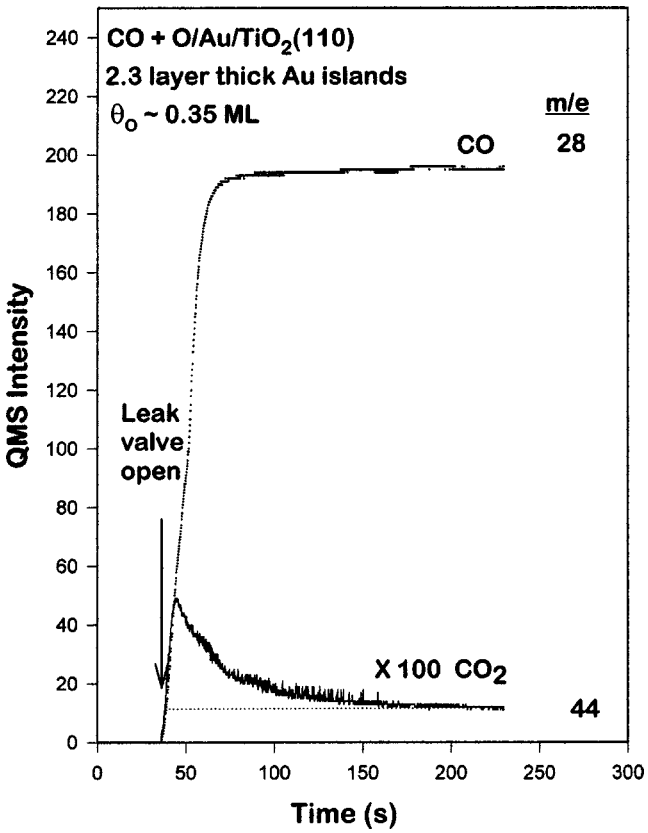

Figure 3. CO_2 evolution upon exposing the Au/TiO_2(110) surface with 0.35 ML pre-adsorbed oxygen to 3.4×10^{-6} mbar of CO at a constant leak rate to initiate the reaction: $CO_g + O_a \rightarrow CO_{2,g}$. The time at which the CO was introduced is indicated by an arrow. The CO signal is also shown.

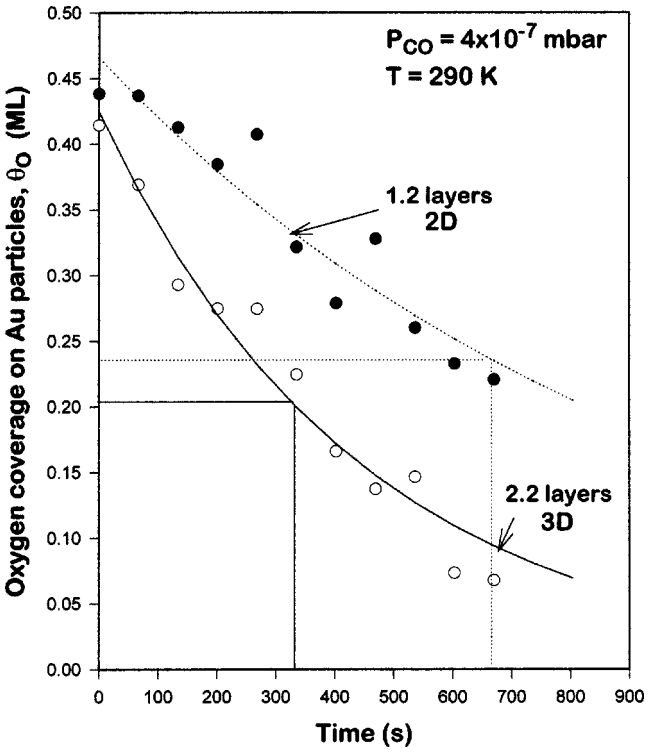

Figure 4. Titration curves of the oxygen coverage versus time in CO gas from figure 2. The half-life of O_a on the ~1-atom-thick (2D) islands is approximately twice that on the 2-atom-thick (3D) islands.

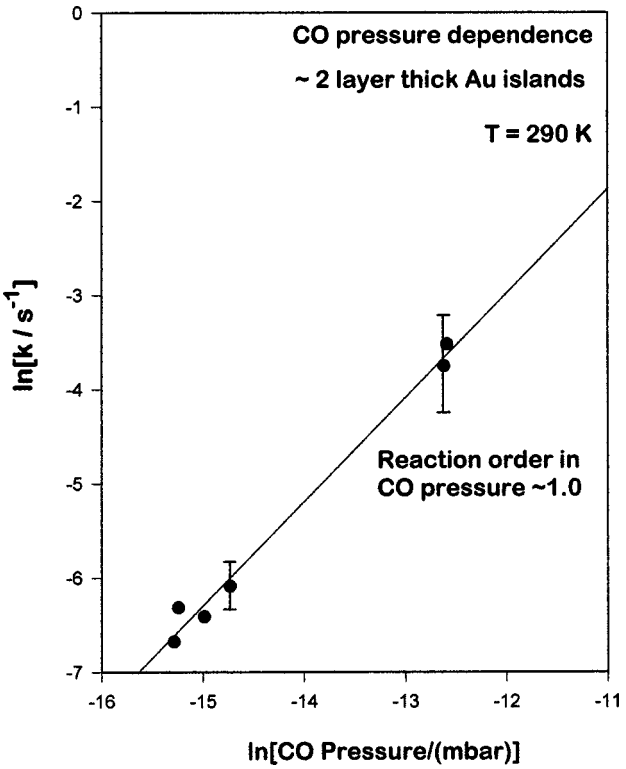

Figure 5. Dependence of the titration rate constant at room temperature on CO pressure. The Au islands used here were ~2-atomic layers thick.

is similar to what has been observed with similar experiments on bulk Au(110) surfaces at room temperature [23]. Initially, the CO_2 evolved at a high rate and decayed exponentially as oxygen adatoms were consumed. At equivalent doses of CO the LEIS Au signal indicated a small fraction of O_a remaining at the end of the experiment (i.e., after following the transient responses of CO and CO_2 with a mass spectrometer), which agreed well with the results of following the titration reaction only with LEIS after the same CO exposure.

Figure 4 shows the room temperature titration curves, or plots of the adsorbed oxygen coverage (on Au particles only) versus time of CO exposure, for 2D and 3D Au particles on TiO_2. The oxygen coverage was derived from Au LEIS measurements such as in figure 2. The full and dotted lines show the exponential fit to the data. The good fit indicates a reaction which is first order in oxygen coverage (θ_O). The first-order rate constant, k, for the decay in the oxygen coverage, as defined by $d\theta_O/dt = -k\theta_O$, was found from the exponential fits to be 0.0010 s^{-1} for 2D islands and 0.0023 s^{-1} for 3D islands of figure 4. We observed generally a slower reaction rate on the O-covered 2D islands than on the 3D particles. The half-life of the oxygen decay on the 2D Au islands was 2.3 times that on 3D islands. The half-life remained nearly constant for thickness of 3D Au islands from 2.2 layers up to ~4 layers. Therefore, only the result for 2.2 layers is shown here. This suggests that the titration rate over these Au/TiO_2 catalysts is dependent on the film morphology, but only changes when the thickness of the Au island decreases below 2 layers.

Figure 5 shows the effect of CO pressure on the titration rate at room temperature for 2-layer-thick Au islands. The CO pressures were varied between 2.3×10^{-7} and 3.4×10^{-6} mbar. From the measured variation of oxygen coverage, θ_O, as a function of time (t), the first-order rate constant, k, was determined at each CO pressure. Figure 5 shows a plot of $\ln k$ versus $\ln P_{CO}$, which should give a straight line the slope of which is the reaction order in P_{CO}. The observed slope of 1.1 ± 0.1 shows the rate of CO production to be nearly first order in CO pressure, similar to that found in CO titration of O_a on bulk Cu(110) [23]. This CO reaction order is much higher than the values of 0.05 and 0.4 reported by Haruta et al. [1] and Bollinger et al. [4], respectively, for quasi-steady-state catalysis. This would suggest that oxygen adsorption is probably the rate-determining step in quasi-steady-state catalysis (so the rate is high order in O_2 and low order in CO), whereas in our transient titration, oxygen adsorption does not play a role, and the rate is proportional to the CO coverage (and thus CO pressure, see below).

Figure 6 shows the first-order reaction rate constant, k, as a function of Au island thickness, at a fixed P_{CO}, as determined from data such as shown in figure 4. The reactivity of oxygen on the Au/TiO_2 catalyst increases as the islands thicken from 2D to 3D islands, but saturates already at average Au island thickness of ~2-atomic layers. For a Au island thickness of ~2-atomic layers, we calculate an initial rate and reaction probabilty per CO collision with the Au

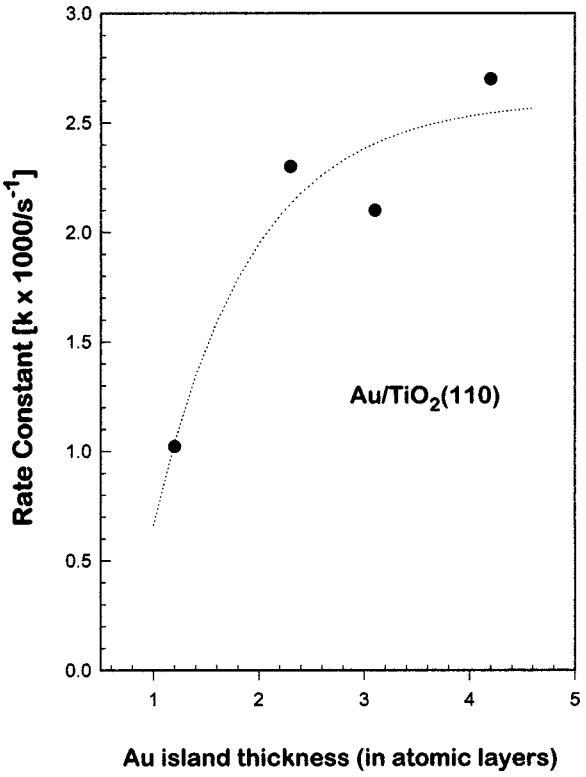

Figure 6. The rate constant of CO titration of O_a as a function Au island thickness at room temperature (293 K). The initial rate is expressed as CO_2 molecules per site per second, where one site is taken as the Au area required for one oxygen adatom at 1.0 ML coverage (∼1.0 Au surface atoms).

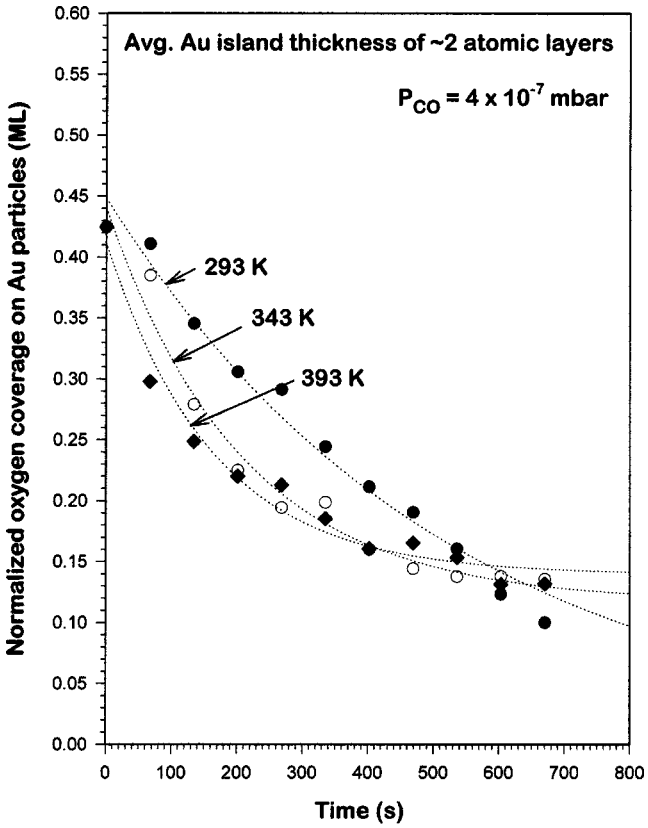

Figure 7. Kinetic plots of the oxygen coverage versus time of CO exposures ($P_{CO} = 4 \times 10^{-7}$ mbar) at three different temperatures. The Au/TiO_2 catalyst was briefly pre-annealed at 423 K before depositing the O adatoms and the subsequent CO titration experiments to minimize the effects of particle sintering. The dashed curves show the exponential decay fits used to determine the first-order rate constant, k. (A baseline offset was included to compensate for the effects of particle sintering.)

surface area of ∼0.001 molecules per site per second and ∼0.013, respectively. These initial rates reported here were obtained from the initial slope of the best-fit exponential decays. These values are similar to the estimated values from the results by Outka et al. [24] for CO titration experiments on O-covered bulk Au(110). However, at an equivalent Au island thickness on TiO_2, Valden et al. [13] reported a TOF of 4 molecules per site per second, from which we estimate a reaction probability per CO collision of $\sim 2.4 \times 10^{-6}$. This large difference proves that the coverage of O_a under the quasi-steady-state reaction conditions ($CO_g + O_{2,g}$) of Valden et al. must be very low (~ 0.4 ML $\times\ 2.4 \times 10^{-6}$–$1.3 \times 10^{-2} \approx 7.4 \times 10^{-5}$ ML, assuming a rate that is first order in θ_O, as shown above). This again suggests that O_2 adsorption is the rate-determining step in quasi-steady-state catalytic CO oxidation from $CO + O_2$.

Figure 7 shows the kinetic plots of the normalized oxygen coverage versus time of CO exposure at various substrate temperatures for Au particles which are ∼2 layers thick. After the initial Au deposition the catalyst was pre-annealed before adsorbing O adatoms or titrating with CO. This was to eliminate any effects of thermal thickening of the Au particles during the subsequent temperature-dependent titrations with CO. Figure 8 shows the corresponding Arrhenius plot of the $\ln k$ versus $1/\text{temperature}$ from the data of figure 7. From this plot we measure a low apparent activation energy of 11.4 ± 2.8 kJ/mol for 2-atom-thick Au particles, which is very close to the bulk value (8.4 ± 4.2 kJ/mol) reported by Outka and Madix [24] on Au(110). It is slightly less than the apparent activation energy of ∼16.7 kJ/mol reported by Valden et al. [13] for the quasi-steady-state $CO + O_2$ catalytic reaction on Au/TiO_2. Note that θ_O in the high-temperature curves does not decay to zero at long time. This is an artifact due to particle sintering during the course of the titration: the loss of Au island area leads to an overestimate of θ_O based on the Au LEIS intensity.

4. Discussion

4.1. TPD results of O adatoms on Au/TiO2(110)

By exposing bulk Au(111) to ozone at room temperature, Saliba et al. [22] reported an oxygen TPD peak temperature of 550 K for O_a coverages of ∼0.5 ML. Sault et al. [6], also using a hot filament to generate atomic oxygen on Au(110)-(1 × 2), reported an O_2 TPD peak at ∼590 K. Certainly differences in the way thermocouples are mounted could lead to variations in the desorption temperature measurements. Nevertheless, the lowest

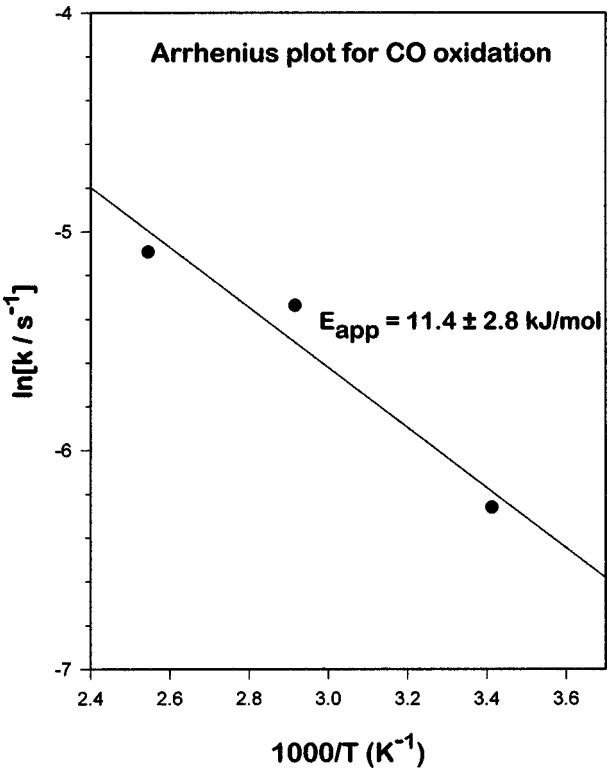

Figure 8. Arrhenius plot of the $\ln k$ from the curves in figure 7 versus $1/$temperature to yield the apparent activation energy for the reaction: $CO_g + O_a \rightarrow CO_{2,g}$.

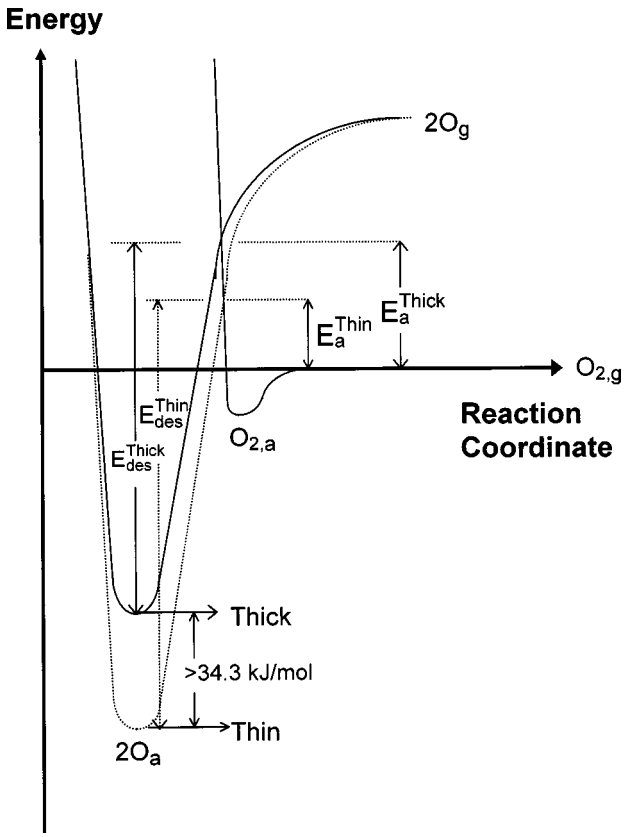

Figure 9. Potential energy diagram for the interaction of oxygen with thin (2D, - - -) and thick (3D, —) Au islands on TiO_2: $E_a^{Thin} < E_a^{Thick}$.

peak temperature we observe at ∼545 K for gold islands that are 6 atoms thick is more in agreement with [22] for Au(111), which indicates that the chemisorption behavior of these Au particles (6 atoms thick) approach that of bulk Au(111). The observation of decreasing temperatures for TPD peaks with increasing island thickness is reminiscent of the behavior of CO desorption from metal islands in several metal on oxide systems [25–27]. We attribute the higher O_2 desorption peak observed for thin Au particles as due to the effect of the underlying TiO_2 substrate on the stability of the oxygen adatoms. Using simple Redhead analysis [28] and assuming first-order desorption kinetics and a pre-exponential factor for desorption of 5.5×10^{12} s^{-1} from a closely related O/Au system [22], we estimate desorption activation energies ranging from 124.7 kJ/mol (for the ∼1-atom-thick islands) to 90.4 kJ/mol (for the 6-atom-thick islands). Since the activation energy for desorption generally follows the same trend as the adsorption energy (and they are equal for non-activated adsorption), we conclude that the ∼34.3 kJ/mol higher activation energy on the thinnest particles corresponds to a larger adsorption energy (i.e., considerably more stable O_a) on the thinnest particles of Au.

Based on prior studies with 2D metal islands on oxide surfaces, it is easy to understand that oxygen bonds more strongly to the 2D Au islands than to 3D islands. In general, 2D islands of late transition metals on oxides chemisorb species more strongly than annealed 3D islands [26,27]. This is attributed to the weaker bonding of the metal to the oxide below (compared to the 3D case where another layer of metal is below). The weaker bonding of Au to TiO_2 compared to Au bonding to Au was confirmed in the present case by the *irreversible* thickening the islands undergo upon annealing in vacuum: 2D islands convert irreversibly into 3D islands that cover less of the surface [15]. The weaker bonding of Au in 2D islands to the layer below (TiO_2) leaves the Au atoms more aggressive in their bonding to adsorbates from above, according to the priniciple of bond energy–bond order conservation [26,27].

Figure 9 helps demonstrate how Brønsted (or linear free energy) relationships [18] predict that the activation barrier for dissociative adsorption of O_2 should be lower for gold particles with a higher adsorption energy for oxygen adatoms. First, we observed an activation energy for desorption of $2O_a$ on 2D Au islands (E_{des}^{Thin}), which is ∼34.3 kJ/mol larger than that for thick Au islands (E_{des}^{Thick}), as shown. This implies that $2O_a$ on 2D Au islands must be more than 34.3 kJ/mol more stable than $2O_a$ on thick islands, since part of this stability difference must also appear at the activation barrier for O_2 adsorption: $E_a^{Thin} < E_a^{Thick}$. This is obvious in the energy diagram, and also argued by the principles of linear free energy relationships [18]. Thus, ultrathin gold particles should be able to dissociatively adsorb O_2 more readily than large gold particles. Since dissociative adsorption of O_2 is immeasurably slow or impos-

sible on pure, bulk gold surfaces [5,6], we postulate that the unusual low-temperature catalytic activity in CO oxidation demonstrated by thin (small) Au particles on TiO_2 is related to the positive influence this stronger bonding to oxygen will no doubt have on the dissociative adsorption rate of O_2.

We have tried but been unable to experimentally demonstrate this by dosing O_2 in the high pressure cell, since the rate of O_2 adsorption is very slow in any case (and possibly rate limiting in the catalytic process). Under high O_2 pressure (250 mbar) exposure conditions where we should have observed it, the adsorbed oxygen would have been rapidly cleaned off by reactions with low-level background impurities. We have shown, for example from CO titration experiments, that CO gas at a partial pressure of only $\sim 10^{-7}$ mbar is sufficient to clean off the O_a as CO_2 in less than $\sim$5 min, so a few ppm of CO in the O_2 in the high-pressure cell would disallow build-up of significant O_a coverage. We are now striving to make the measurement in a cleaner environment.

4.2. Titration experiments: $CO_g + O_a \rightarrow CO_{2,g}$

This reaction is extremely rapid at room temperature, and its rate increases as island thickness increases. Thus, the association reaction ($CO_g + O_a \rightarrow CO_{2,g}$) gets faster as the oxygen adsorption energy decreases, again as expected based on Brønsted relations.

The kinetics of CO titration of O_a from thin (2D) and thick (3D) Au islands is understandable with the potential energy diagram shown in figure 10. Assuming the Langmuir–Hinshelwood (LH) mechanism proposed for this reaction [2,4], the overall titration rate, R_{LH}, can be written as [23]

$$R_{\mathrm{LH}} = \frac{\nu \exp\{-(E_{\mathrm{LH}} + \Delta H_{\mathrm{ad}}^{\mathrm{CO}})\}}{RTP_{\mathrm{CO}}\theta_{\mathrm{O}}}, \qquad (1)$$

where E_{LH} is the activation energy for the Langmuir–Hinshelwood step: $CO_a + O_a \rightarrow CO_{2,g}$, $\Delta H_{\mathrm{ad}}^{\mathrm{CO}}$ is the adsorption enthalpy associated with the step: $CO_g \rightleftharpoons CO_a$ (here it is assumed that the CO coverage is low and this step is in rapid equilibrium) and ν is the pre-exponential factor for the overall net reaction rate. Note that this expression gives properly the observed first-order dependencies on P_{CO} and θ_{O}. In figure 10 we show the effects on the energies of the adsorbed species due to the stronger chemisorption of O_a on thinner Au islands. As noted above, $2O_a$ on 2D islands is >34.3 kJ/mol more stable than on thick islands. Thus, O_a is >17.2 kJ/mol more stable on 2D islands. This energy difference is reflected in the first two states on the left side of figure 10: "$CO_g + O_a$" and "$CO_a + O_a$". Of course, since CO_a is also slightly more stable on thin Au islands than on thick islands [9], the second state ($CO_a + O_a$) should have even a larger difference in stability. Again, linear free energy relationships predict that a fraction of this stability difference will remain at the transition state along the reaction coordinate to the product $CO_{2,g}$. Thus,

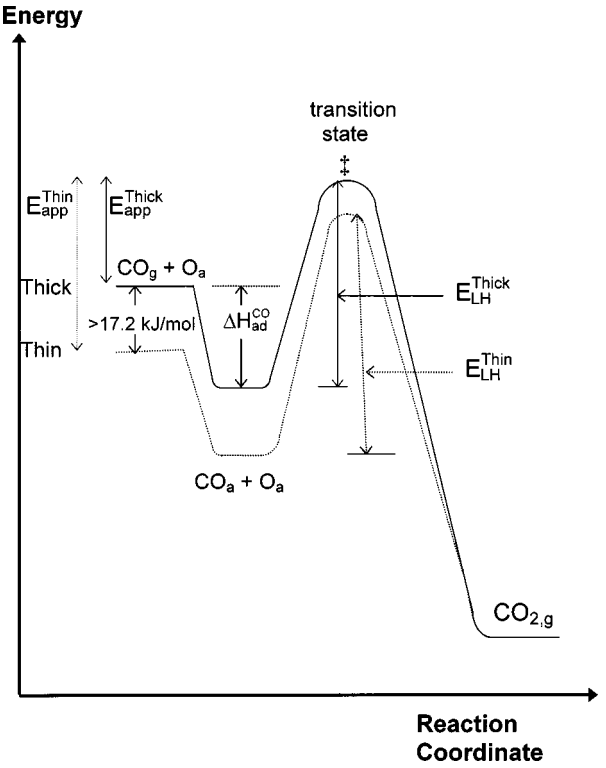

Figure 10. Potential energy diagram illustrating the course of the reaction: $CO_g + O_a \rightarrow CO_{2,g}$ on thin (2D, ---) and thick (3D, —) Au islands on TiO_2. The effect of the island thickness on the overall rate is dominated by the activation energy of the Langmuir–Hinshelwood (LH) step, which in turn is dominated by the O_a stability, such that: $E_{\mathrm{app}}^{\mathrm{Thin}} > E_{\mathrm{app}}^{\mathrm{Thick}}$.

E_{LH} should be larger for thin Au islands than for thick Au islands, as shown. This effect alone would result in a slower rate on thin Au islands according to equation (1), as observed. Let us consider also the effect of $\Delta H_{\mathrm{ad}}^{\mathrm{CO}}$ on the apparent activation energy, $E_{\mathrm{app}} = E_{\mathrm{LH}} + \Delta H_{\mathrm{ad}}^{\mathrm{CO}}$, and the overall rate R_{LH}. The $\Delta H_{\mathrm{ad}}^{\mathrm{CO}}$ is less than -33.5 kJ/mol [24] but it becomes more negative on thinner Au islands [9], thus making the overall rate faster on thinner (2D) Au islands than on thicker (3D) islands according to equation (1). Since the opposite effect is observed, it implies that the effect of island thickness on the overall rate is rather dominated by the effect of island thickness on the activation energy of the LH step, such that $E_{\mathrm{app}}^{\mathrm{Thin}} > E_{\mathrm{app}}^{\mathrm{Thick}}$, as shown in figure 10. This is reasonable, since the effect of $\Delta H_{\mathrm{ad}}^{\mathrm{CO}}$ should be smaller than that of $\Delta H_{\mathrm{ad}}^{\mathrm{O}}$, since the latter is much larger in magnitude. Therefore on thinner Au islands where O adatoms adsorb more strongly, the rate of CO_2 production should proceed less rapidly, as observed. Since the observed rate difference is only a factor of $\sim$2 at 293 K, this requires a difference, $E_{\mathrm{app}}^{\mathrm{Thin}} - E_{\mathrm{app}}^{\mathrm{Thick}}$, of only $\sim$1.7 kJ/mol.

For islands of $\sim$2-atomic layers thickness the titration reaction is found to be extremely fast at room temperature and show a first-order dependence on CO pressure. This indicates that, if the production of oxygen adatoms on the Au particles is one of the elementary steps in the mechanism of low-temperature CO oxidation on this system, then the dissociative adsorption of O_2 must be the rate-limiting

step in this reaction during quasi-steady-state catalysis such as in [1,2,13]. Again for islands of ∼2-atomic layers thickness the titration rate increases slowly with temperature, with an apparent activation energy of 11.4 ± 2.8 kJ/mol as also found on bulk Au(110) [24] which indicates that the catalytic activity of these 2-atom-thick Au particles approaches that of bulk Au in every aspect, except for the differences expected in the rate of dissociative oxygen adsorption discussed above.

Whereas Pt, Rh and Pd catalysts bind CO too strongly, so that at room temperature their surfaces are poisoned by CO against oxygen adsorption, ultrathin islands of Au on TiO_2 have a much, much weaker bond to CO, so that Au sites are still free at room temperature. We postulate that these sites can dissociatively adsorb oxygen, since they bind O_a so much more strongly than bulk Au, thereby allowing room-temperature catalytic oxidation to proceed at steady state. Thus, if the rate at which ultrathin Au islands dissociatively adsorb O_2 can be proven to be as fast as the net rate of low-temperature CO oxidation, then the mechanism for the net reaction must obviously be the same Langmuir–Hinshelwood process followed at higher temperatures by more traditional catalysts (Pt, Pd, Rh).

5. Conclusions

TPD results of oxygen adsorption on Au/TiO_2(110) show substantially higher desorption temperatures and activation energies for ultrathin gold particles on TiO_2(110) than for thick particles. This implies larger heats of oxygen adsorption and faster dissociative O_2 adsorption for ultrathin gold particles.

The rate of titration of oxygen adatoms with CO (to produce CO_2) is first order in CO pressure and oxygen coverage, and is extremely rapid at room temperature. Its rate is slightly lower for the thinnest Au (2D) islands, as expected from Brønsted relations. For islands of ∼2-atom thickness, the rate increases slowly with temperature, with an apparent activation energy of 11.4 ± 2.8 kJ/mol similar to bulk Au(110).

Acknowledgement

The authors would like to thank Henry Ajo for his help in conducting the experiments. We also acknowledge with pleasure the support of this work by the Department of Energy, Office of Basic Energy Sciences, Chemical Sciences Division.

References

[1] M. Haruta, S. Tsubota, T. Kobayashi, H. Kageyama, M.J. Genet and B. Delmon, J. Catal. 144 (1993) 175.
[2] M. Haruta, Catal. Today 36 (1997) 153.
[3] T. Hayashi, K. Tanaka and M. Haruta, J. Catal. 178 (1998) 566.
[4] M.A. Bollinger and M.A. Vannice, Appl. Catal. B 8 (1996) 417.
[5] N.D.S. Canning, D. Outka and R.J. Madix, Surf. Sci. 141 (1984) 240.
[6] A.G. Sault, R.J. Madix and C.T. Campbell, Surf. Sci. 169 (1986) 347.
[7] M.A. Dekkers, M.J. Lippits and B.E. Nieuwenhuys, Catal. Lett. 56 (1998) 195.
[8] F. Boccuzzi, A. Chiorino, S. Tsubota and M. Haruta, Catal. Lett. 29 (1994) 225.
[9] Z.M. Liu and M.A. Vannice, Catal. Lett. 43 (1997) 51.
[10] L. Zhang, R. Persaud and T.E. Madey, Phys. Rev. B 56 (1997) 10549.
[11] J.-D. Grunwaldt and A. Baiker, J. Phys. Chem. B 103 (1999) 1002.
[12] M. Okumura, S. Nakamura, S. Tsubota, T. Nakamura, M. Azuma and M. Haruta, Catal. Lett. 51 (1998) 53.
[13] M. Valden, S. Pak, X. Lai and D.W. Goodman, Catal. Lett. 56 (1998) 7.
[14] M. Valden, X. Lai and D.W. Goodman, Science 281 (1998) 1647.
[15] S.C. Parker, A.W. Grant, V.A. Bondzie and C.T. Campbell, Surf. Sci., in press.
[16] C. Xu, W.S. Oh, G. Liu, D.Y. Kim and D.W. Goodman, J. Vac. Sci. Technol. A 15 (1997) 1261.
[17] V.A. Bondzie, S.C. Parker and C.T. Campbell, J. Vac. Sci. Technol. A 17 (1999) 1717.
[18] W.C. Gardiner, Jr., *Rates and Mechanisms of Chemical Reactions* (Benjamin, Menlo Park, CA, 1972) p. 163.
[19] C.T. Campbell and M.T. Paffett, Surf. Sci. 139 (1984) 396.
[20] C.T. Campbell, Surf. Sci. 157 (1985) 43.
[21] L. Gamble, M.A. Henderson and C.T. Campbell, J. Phys. Chem. 102 (1998) 4536.
[22] N. Saliba, D.H. Parker and B.E. Koel, Surf. Sci. 410 (1998) 270.
[23] M.E. Domagala and C.T. Campbell, Catal. Lett. 9 (1991) 65.
[24] D.A. Outka and R.J. Madix, Surf. Sci. 179 (1987) 351.
[25] H.-J. Freund, B. Dillman, D. Ehrlich, M. Habel, R.M. Jaeger, H. Kuhlenbeck, C.A. Ventrice, F. Winkelmann, S. Wohlrab and C. Xu, J. Mol. Catal. 82 (1993) 143.
[26] C.T. Campbell, Surf. Sci. Rep. 27 (1997) 1.
[27] C.T. Campbell, Curr. Opin. Solid State Mater. Sci. 3 (1998) 439.
[28] P.A. Redhead, Vacuum 12 (1962) 203.